RESEARCH

Open Access

Children's cloth face mask sizing and digital fit analysis: method development

Mona Maher[1], Jenny Leigh Du Puis[1], Katarina Goodge[1], Margaret Frey[1], Heeju Terry Park[1] and Fatma Baytar[1*]

*Correspondence:
fb38@cornell.edu

[1] Department of Human Centered Design, College of Human Ecology, Cornell University, 37 Forest Home Dr., 133 Human Ecology Building, Ithaca, NY 14853-4401, USA

Abstract

There is a necessity to use digital data and tools when developing children's products. The present study was designed to provide digital methods to guide product development and problem-solving when using 3D body scans and face mask simulations for 6-year-olds. First, key facial measurements were evaluated to better understand the variables that might affect face mask sizing for children for the selected age group. Then the findings were used to optimize the size and fit of a cloth face mask design. Next, the fit of the digital, optimized face mask design was tested on 44 head scans from Size North America by using subjective and objective fit assessment techniques. Study findings suggested that width and length-related measurements are critical for children's face masks. Body mass index (BMI) and ethnicity were also found to be the main factors for identifying size ranges in the selected age group. As BMIs increase, face mask sizes should increase. Additionally, the results indicated a need to use a larger database of children of all ethnicities to design an inclusive facemask that would provide a comfortable and protective fit for different facial proportions. Although the results cannot be generalized due to the case study approach of the present research and its focus on methods development, they can provide manufacturers, designers, and researchers with guidelines on how to develop proper sizing and use digital data to conduct functional fit analysis for facemasks.

Keywords: Cloth face mask, Children, Sizing, 3D body scanning, Virtual fit

Introduction

Face masks are essential preventive measures to reduce airborne transmissions of respiratory viruses, such as SARS-CoV-2 (Centers for Disease Control and Prevention [CDC], 2022). Their effectiveness increases especially when they fit snugly and comfortably on the face (CDC, n.d.; Smart et al., 2020). Commercially available children's cloth masks range widely in material type, fabric structures, construction, layering, and shape (Du Puis et al., 2022). Even though many face mask designs exist on the market (Du Puis et al., 2022), there is a lack of anthropometric data, and as a result lack of suggestions for sizing to provide the best face mask fit for children. A previous study indicated that children's lower breathing resistance, compared with adults, necessitates the selection of proper fabrics and a layering system that ensures efficient filtration while providing optimal comfort during prolonged mask usage and minimizing the risk of respiratory strain in children (Goodge et al., 2022). Therefore, it is crucial that face masks are specifically designed for children. Several studies highlighted the important landmarks and measurements for improving the fit of medical or pediatric face masks (Amirav et al., 2014; Fu & Luximon, 2019; Goto et al., 2015; Lee & Lee, 2021; Seo et al., 2017), but these findings have not been fully applied to cloth face masks for children.

Children's face and head proportions differ significantly from adults' (Farkas et al., 1992; Lin et al., 2010). For instance, the nose and eyes, in addition to facial length, width, and volume increase from childhood to adulthood (Ferrario et al., 1998). For this reason, face masks that are designed for adults and sized down to fit smaller faces may not fit children as expected, thus compromising their protective quality. Therefore, designing a face mask based on children's anthropometric data is important to provide well-fitted cloth face masks. Additionally, because virtual product development is becoming more prominent in the industry (Gill, 2015), there is a need to establish guidelines for each specific product type.

Children's facial anthropometry and face wear sizing

Commercial cloth face masks for children are available in different shapes as well as dimensions and typically include sized-down versions of adult face masks. However, masks produced for adults may not seal well on children's faces (3M, 2021). Anthropometry plays a significant role in developing properly fitted head and face wear including face masks. 3D scanning technologies are widely used tools to provide accurate and reliable anthropometric data, improve design, and ensure fit and protection (Conkle et al., 2019). Recent studies that used 3D scanning to study the growth pattern of heads and faces among children showed statistically significant differences in the head and face growth patterns between girls and boys with different ethnicities, ages, and BMIs (Fu et al., 2019; Goto et al., 2019; Napolitano et al., 2017; Seo et al., 2017). Moreover, they indicated that key facial anthropometric landmarks could help develop better-fitting face masks as well as identify size groups to provide coverage for more people.

An analysis of anthropometric data sets of children younger than 7 years old for the design of ventilation masks revealed that two prominent component factors, i.e., facial width and height, could explain about 70% of facial variations among Dutch children (Goto et al., 2015). Researchers studied facial width- and height-related measurements and suggested three size groups (small, medium, and large) for classifying children's facial measurements (Amirav et al., 2014; Seo et al., 2017). In a study of Korean children's facial anthropometry (Seo et al., 2017), researchers included angles and curvature lengths in addition to the widths and lengths measurements. Participants' facial measurements, shapes, and sizes were classified into small, medium, and large size groups (Seo et al., 2017). To investigate the growth pattern of the head and face of Chinese children, five landmarks (on both left and right sides), including glabella, nasion, gnathion, and frontotemporal (left and right) were positioned to measure six facial dimensions (i.e., head circumference, head length, head width, forehead width, face height, and morphological face height) (Fu et al., 2019). In another study, 15 landmarks (i.e., glabella, sellion, endocanthion (left/right), nasal root point(left/right), pronasale, alare (left/right), subnasale, cheilion(left/right), sublabiale, pogonion, and menton) were used for measuring five facial dimensions (Goto et al., 2019). Instituto de Biomecánica de Valencia

(IBV) collaborated with Asociación Española de Normalización (UNE) to establish the minimum requirements for developing non-reusable hygienic masks for children, aged 3–12 years old (Spanish Association for Standardization, 2020). For this purpose, IBV used 3D anthropometric data from over 1000 children including two widths (i.e., tragion and cheekbone) and one length (i.e., sellion to chin) landmarks and recommended pediatric mask patterns in three sizes based on ages: small (3–5 years), medium (6–9 years) and large (10–12 years) (Asociacion RUVID, 2020).

Even though the results from these studies highlighted the important landmarks and measurements for developing medical or pediatric face masks, there is still a lack of studies to understand how cloth face mask patterns relate to facial landmarks to provide good coverage for children, and how they should be sized based on children' growth patterns. Recently, the American Association of Textile Chemists and Colorists (AATCC) M14-2020 has indicated that good fit for adult cloth face masks is related to the following key facial measurements including bigonial breadth, bitragion chin arc, bizygomatic breadth, bitragion subnasale arc, interpupillary breadth, and menton-sellion length (AATCC, 2020). This brings an insight into the understanding of the variability of these key factors among children and how to translate this information into product sizes for children's cloth face mask design. The significant measurement differences among children as they grow up should be considered in the design of children's products because both CDC and the American Academy of Pediatrics (AAP) (2022) recommended wearing well-fitting face masks, which must cover the mouth and nose and fit snugly along the side of the face without any gaps.

Children's cloth face mask fit and fit evaluation approaches

The fit of a facemask is as important as the effectiveness of its materials for protection (Du Puis et al., 2022). During the initial stage of the COVID-19 pandemic there was a surge in the home and community production to make cloth face masks, which were worn more frequently than nonwoven facemasks (Snyder et al., 2020). CDC advised the wearing of cloth face masks for individuals over the age of 2, and for those whom the wearing of masks would not impede medical issues. Although AATCC released M14-2020 as a guiding document for non-medical face coverings in 2020 and the American Society for Testing and Materials (ASTM) published the F3502-21 standard for Barrier Face Coverings in 2021 for adults, children were excluded from these documents, which limited the opportunity to protect this vulnerable group. An earlier study analyzed facial respirator shapes using 3D anthropometric data and defined good fit as a relatively small total distance between the face and the mask's landmark points (Fenlon, 2007). In that study, achieving the optimum sealing between face wear and face was explained as another factor for providing a good fit. Related to cloth face coverings, AATCC M14-2020 defined a well-fitted mask as fully covering the user's nose and mouth while fitting snugly against the side of the face without gaps or causing difficulty breathing.

In general, a good fit for garments means pleasing proportions, no constriction of the body, and adequate ease of movement without leading to gaping. Grain, ease, line, balance, and set are the key factors that impact garment fit (Erwin et al., 1979). These factors can be evaluated subjectively by the wearer or a team of fit experts (Fan et al., 2004), or objectively by quantifying garment fit from 3D scans (Loker et al., 2005). For objective fit analysis, 3D scans wearing underwear or tight-fitting garments (also called "minimal" scans) are merged with scans wearing garments, and distances (i.e., ease amounts) between the clothed scan and minimal scan are measured (Ashdown et al., 2004). The same approach can be used when assessing the fit of face wear. Compared with a real human head, digital head forms do not go through weight changes or fatigue over time. These head forms can be re-analyzed if additional measurements are required and as their accessibility increases verification and validation of the measurements. In addition, they can provide volumetric and contour data. For example, NIOSH researchers used head and face anthropometric data as well as 3D scans for developing new head forms in five size categories small, medium, large, long/narrow, and short/wide (Zhuang et al., 2010). Additionally, digital head forms can be 3D printed for objective and subjective fit evaluations. The study of the redesign of an open-system oxygen face mask for children recommended using 3D scanning technology to improve a mask fit with simulation while utilizing 3D printing technology (Napolitano et al., 2017).

Therefore, the present study aimed to serve as a case study to develop methods for digital product development and testing by using digital humans through analyzing the facial anthropometry of 6-year-old children and laying the groundwork for digital fit assessment of a cloth face mask designed for this age group. To our best knowledge, none of the existing studies explicitly addressed the relationship between cloth face mask patterns and facial landmarks and applied digital technologies to evaluate cloth face mask fit by using subjective and objective techniques. Therefore, the following research questions were examined by narrowing down the age group to 6-year-old children to limit the growth pattern variations to one age group as explained by Goto et al. (2019):

RQ1. What are the key facial measurements when developing a well-fitted cloth face mask for 6-year-old children?

RQ2. Which factors can determine sizing decisions when developing a well-fitted cloth face mask for 6-year-old children?

RQ3. How to evaluate fit when using a virtual prototype of a facemask design on 6-year-old children?

Methods

Selection of the head scan dataset for both anthropometrical data collection and digital fit analysis

Forty-four head scans of 6-year-old children (boys and girls) were used as a dataset. The scans were a subset of a larger database that was captured by a Human Solutions Vitus 3D body scanner during the Size North America project that was ran by Human Solutions from 2017–2018. Human Solutions had consent forms for the participants and parents signed the forms on behalf of their children before body scanning. The company shared the dataset with our research team after anonymizing and de-identifying the data. The scans were analyzed as secondary data. BMI was calculated with the BMI percentile calculator developed by CDC for children and teens (Centers for Disease Control and Prevention, n.d.) and categorized as Underweight, Healthy weight, Overweight, and Obese, accordingly. In the following sections, when describing the scans from this group, the term "digital humans" was used instead of "participants" to emphasize that no human participants were recruited in the present study. Ethnicities were grouped based on the U.S. Census categorization (U.S. Census Bureau, 2022.)

Landmarks

Anthropometric landmarks should be defined to be able to take measurements. To identify facial landmarks on the 3D scans, head scan obj files were imported into Geomagic Wrap 2021. To align the 3D images and landmark coordinates, the position of each subject and the orientation of each of the scans were aligned using a Python script in Geomagic Wrap. The files were landmarked according to the AATCC M14-2020 guideline. Ten landmarks were selected to obtain information on the identifiable facial measurements related to the design of cloth face masks. These landmarks included Tragion (T), the superior point on the juncture of the cartilaginous flap of the ear with the head (left & right); Pronasale (TP), the point of the anterior projection of the tip of the nose; Menton (M), the lowest point in the middle on the lower border of the chin; Infraorbital (I), the lowest point on the anterior border of the bony eye socket (left & right); Gonion (G), most posterior inferior point on the angle of the mandible (left & right); and one-third of the nose length down from the anthropometric Sellion (S) landmark (P), which was selected based on the facemask's sealing point on the nose bridge (Fig. 1). Next, the distances between these landmarks were calculated both in straight (i.e., the shortest distance between two points) and curve lengths (i.e., distances between two points were taken on the surface).

To increase the reliability of the landmark placements, and therefore measurements, as well as to reduce memory bias, each scan was landmarked and measured six times in a minimum of 12 h-intervals. The average differences were kept to an allowable

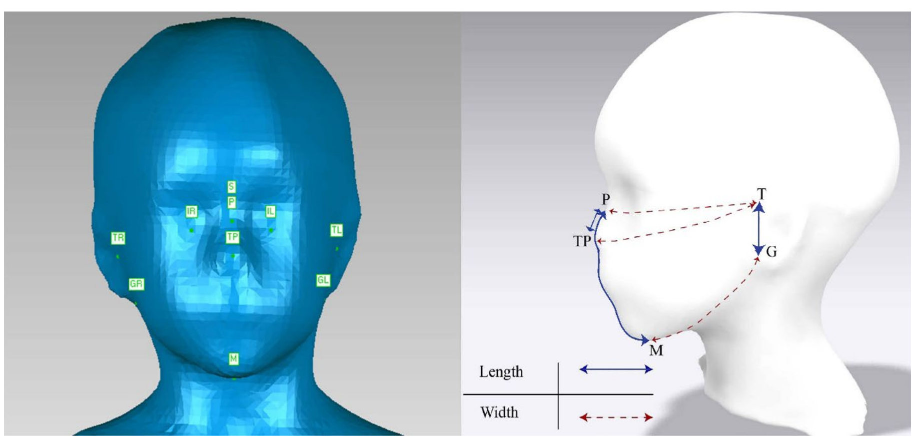

(a) (b)

Fig. 1 **a** Landmark placements on the face and **b** measurements of length (solid lines) and width (dotted lines) taken between the landmarks. Landmarks definitions according to the AATCC14-2020. Sellion (S) (The most posterior midsagittal point on the nasal root at the top of the nasal bridge), P (1/3 of the nose length down from the Sellion anthropometric landmark), Pronasale (TP) (The most anterior midsagittal point of the tip of the nose. It is not an anthropometrical landmark and was selected based on the facemask's sealing point on the nose bridge), Menton (M) the lowest point in the middle on the lower border of the chin, Infraorbital (I) (Left and right. The lowest point on the anterior border of the bony eye socket), Tragion (T) (Left and right. The superior point on the juncture of the cartilaginous flap of the ear with the head), and Gonion (G) (Left and right. The most inferior midsagittal point of mandible) error (2 mm), as defined by Gordon et al. (2014), for all dimensions. Additionally, one head scan was 3D printed, and landmarks were placed on the head form manually. The selection of this 3D-printed model was based on whether the scan had prominent ears that could hold the actual facemask mask on the 3D-printed head form, belonged to the healthy BMI group, and had measurements that were closest to the subset's average measurements. The distances between the landmarks on the 3D printed form were measured five times and compared to the measurements taken in the software to establish consistency and reliability for landmarking and measuring. As a result, 11 measurements were extracted and imported into a Microsoft Excel file for data analysis.

Anthropometric data analysis

For data analysis, descriptive statistics with correlations at 95% confidence level by Principal Component Factor (PCA), Two-step cluster sampling, and one-way ANOVA were conducted in IBM Statistical Package for Social Sciences (SPSS) 27.

Selection of the key measurements through PCA

PCA was applied to transform several possibly correlated variables (i.e., 18 facial measurements) into a smaller number of principal components (PCs.) This study selected Varimax rotation since it could transform the correlated variables into a smaller number of PCs. The decision on the number of components to retain was based on three factors: (1) eigenvalues greater than 1.0, (2) rotated component loadings if a measurement was highly correlated with more than two components, the analysis was re-conducted with this measurement removed, and (3) the number of variables that have a high correlation with each component; each PC should have a minimum of three variables in practice. Otherwise, that component was removed from the data analysis.

Digital humans' classification through two-step cluster sampling

A two-step cluster analysis was conducted using the PC scores as independent variables to assign digital humans to several clusters where a set of specified variables determined similarities. To analyze whether clusters were significantly different from one another, each body measurement was compared through one-way ANOVA.

Fit evaluation of the novel face mask design

After developing the physical prototype of the novel face mask design and perfecting its fit on the 3D head form (Du Puis et al., 2022), its patterns were digitized into Optitex PDS. The findings on the key facial measurements as well as PCA and Two-step cluster sampling were used to modify pattern measurements to improve the fit of the face mask. Patterns were not custom-made for 44 digital humans but were modified based on the identified clusters' characteristics and their measurements. The final patterns were imported to Clo3D software for virtual fit analysis (Fig. 2). Simulations were created based on the material specifications for the selected fabrics that were validated in a previous study (Goodge et al., 2022). Because children have lower breathing resistance than adults, when designing the face mask it was considered that good fit should provide acceptable air permeability without sacrificing the filtration efficiency so that the facemask would be both effective and not put stress on the child's respiratory system (Fig. 2).

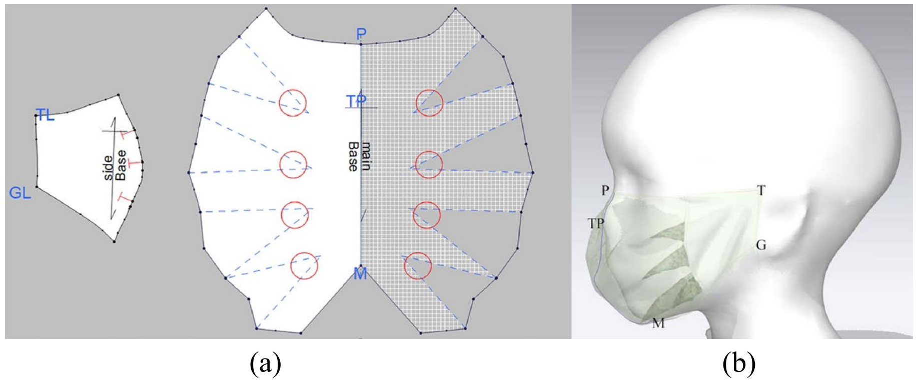

Fig. 2 **a** Patterns for the novel facemask and **b** digital facemask alignment at the landmarks. During facemask patternmaking, dart intakes were used to create pleats. In Optitex PDS, the red circles on the darts indicate the location of the drill holes, which remain on the digital patterns by default

In general, virtual models are used to supplement human wear trials during fit testing and are not utilized in the final stage of product development (Weatherbed, 2023). Due to the limitation of recruiting children during the Covid-19 pandemic, and the necessity of using digital models to better visualize the alignment of face landmarks with the facemask patterns' landmarks, fit evaluations took place digitally by using head scans and virtual face mask simulations. Digital face masks were created in Clo3D by using the fabric properties measured for the actual face mask. The patterns were stitched digitally; placed on the faces, and pinned at the P, T, G, and M landmarks to imitate securing with nose wires and ear loops. To mimic the face mask's inner silicone edges' sealing function, the edges of the digital face mask were stabilized on the face by setting the skin offset to 0.00 mm. To validate the digital face mask fit process against a physical sample, a six-year-old boy who was the son of one of the authors was recruited to try on the physical prototype. He donned the face mask and was scanned in the Human Solutions Vitus Head 3D scanner. The scans of the human participant wearing the actual face mask were taken as a basis when simulating the face mask on the same human participant's head scan. After validating the fit resemblance, settings, and steps related to the virtual fitting procedures were kept the same for the rest of the digital samples.

The fit of the digital masks was evaluated both objectively by taking measurements between the face and mask (i.e., ease) at the sagittal plane (Fig. 3) and subjectively by visually examining both set, i.e., draglines, and ease. Using these two approaches helped in identifying the acceptable fit levels and associating them with metrics related to the specific topic and target group of this study. Scans wearing the digital masks were exported as obj files, which were then imported to Geomagic Wrap 2021 for quantifying the distances (ease) between the face and the prototype face mask at the nose tip and mouth levels. In the sagittal view, vertical planes were placed at the tip of the nose and mouth opening (Fig. 3). The distances between the two planes were calculated in Geomagic Wrap 2021.

Because the face mask's silicone edges allowed it to stick to the face, the fit was evaluated objectively by measuring the distance, or ease amounts, between the face mask and the face at the nose and mouth levels. Fabric opacity was set to 30 out of 100 to subjectively assess the fit at the nose and mouth levels. Research by Ashdown et al. (2005) showed that two

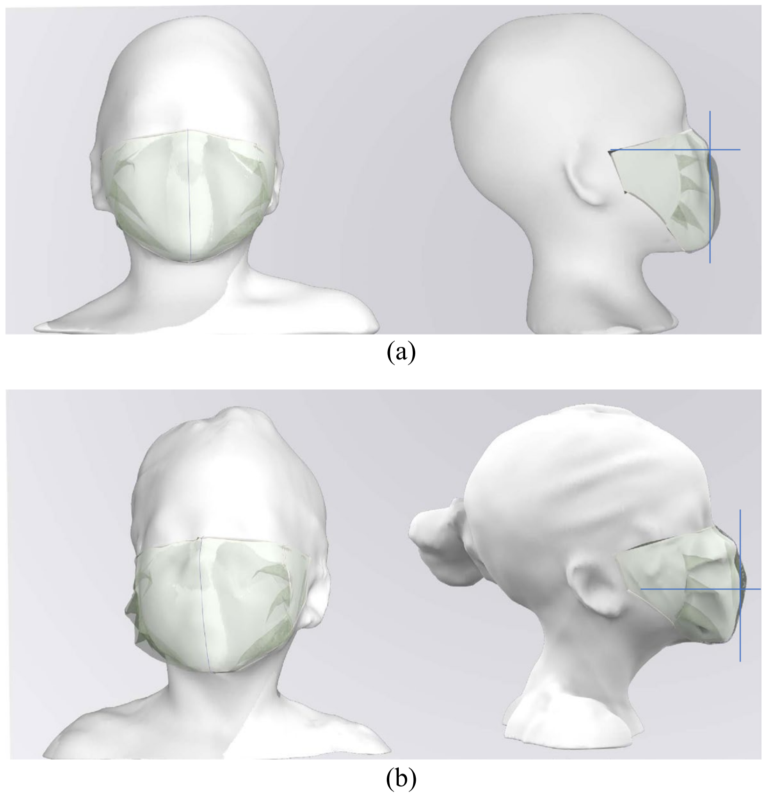

Fig. 3 Examples of tight fit at the **a** nose and **b** mouth levels

fit experts are enough to make a reliable fit analysis. Therefore, two judges with more than 10 years of experience in pattern making, 3D body scanning, and virtual prototyping evaluated fit by viewing the front, left, and right sides of the face mask prototype, and rated fit at two locations (i.e., nose and mouth levels). First, the fit of the physical and virtual facemasks was analyzed on a six-year-old boy, who was in the healthy BMI group and from one of the researchers' family. This activity was conducted to establish a baseline for the digital face mask, therefore did not require IRB review. Then, in a random order, each scan wearing the face mask was carefully examined by rotating them as well as zooming in and out. A 2-point Likert-type scale was used to rate the facemask fit with the following labels: 1 = not acceptable fit (too tight/close to face at both locations), 2 = acceptable fit (there is sufficient ease at both locations and no sign of extreme tightness/looseness) (Fig. 3). Pearson's Chi-squared test was used to determine whether there was a statistically significant association between fit and digital humans' BMI, ethnicity, and sex. Descriptive statistics and one-way ANOVA were calculated in SPSS v.27 to compare the fit rates based on the digital humans' BMI, sex, and ethnicity. The findings were reported in the following Results section and then their explanations and interpretations were given in the Discussion section.

Results

Demographics

A total of 44 scans of 6-year-old children were used for data analysis. Fifty-seven percent of the digital humans were girls (n = 25) and 43% of them were boys (n = 19). Most of the digital humans were White (n = 22, 50%), followed by Asian (n = 12, 27%), and Black/African American (n = 10, 23%). Digital humans' BMIs were distributed as follows: Underweight (n = 3, 7%), Healthy weight (n = 27, 61%), Overweight (n = 7, 16%), and Obese (n = 7, 16%). Detailed demographic information was given in Table 1.

Anthropometric data analysis

Selection of key face measurements

To examine RQ1, PCA was conducted using eight width-, and three length-related facial measurements. The total amount of variables in the sample was 11. Four PCs with eigenvalues greater than 1.0 were extracted. The PCA shows that 83.21% of the variation among 11 variables was explained by four PCs.

As presented in Table 2, the first PC had high loadings on three length measurements (i.e., TP-P, P-M, T-G) and two width measurements (i.e., $|T_{Right} - T_{Left}|$, $|G_{Right} - G_{Left}|$). The second PC loaded highly on two width measurements (i.e., P-T, T-TP) and one length measurement (M-G). The third PC had high loadings on two width measurements ($|I_{Right} - I_{Left}|$, I-P). The last PC loaded highly on three width measurements ($|T_{Right} - T_{Left}|$, $|I_{Right} - I_{Left}|$, and $|G_{Right} - G_{Left}|$), which were highly correlated with two PCs. After removing these measurements, PCA was run one more time with the remaining variables. As a result, three PCs with eigenvalues greater than 1.0 had high load variables (Table 3).

The total variance explained by these eight variables was 72.21%. Eigenvalues for all three PCs were greater than 1.0, but only the first two PCs, PC1 (33.5%), and PC2 (27.12%) were found to make a strong contribution to the variance explained. In addition, PC3 had fewer than three variables, which was not enough to provide adequate information about that component. Therefore, only the first two PCs were selected as true PCs. Besides, PC1 included two widths (P-T, T-TP) and one length (T-G) measurements. PC2 included two lengths (TP-P, P-M), and one width (M-G) measurements. Because of the high correlation between the length and width measurements in each PC,

Table 1 Digital humans' BMI distributions based on sex and ethnicity

		Mean [kg/m^2]	SD [kg/m^2]	n $_{Female}$	n $_{Male}$	n $_{Total}$
$BMI_{Healthy\ Weight}$		15.17	0.43	15	12	27
Ethnicity	Asian	15.08	0.99	6	2	8
	Black/African American	15.18	0.38	2	4	6
	White	15.23	0.72	7	6	13
BMI_{Obese}		19.85	0.61	3	4	7
Ethnicity	Asian	18.50	0.28	0	2	2
	Black/African American	20.1	0.42	1	1	2
	White	20.60	0.50	2	1	3
$BMI_{Overweight}$		17.72	0.44	5	2	7
Ethnicity	Black/African American	18.35	0.21	2	0	2
	White	17.48	0.10	3	2	5
$BMI_{Underweight}$		12.43	0.85	2	1	3
Ethnicity	Asian	11.85	0.19	2	0	2
	White	13.30	n/a	0	1	1
	n_{Total}			25	19	44

Table 2 Rotated component matrix

Key variables	Component			
	1	2	3	4
Pronasale (TP)-P	**0.842**	− 0.177	0.047	0.071
P-Tragion (T)	− 0.009	**0.959**	0.136	0.154
Tragion (T)$_{\text{Right}-\text{Left}}$	**0.651**	0.311	− 0.134	**0.801**
Infraorbital (I)$_{\text{Right}-\text{Left}}$	0.079	0.092	**0.693**	**0.796**
Infraorbital (I)-P	0.074	0.101	**0.973**	0.089
P-Menton (M)	**0.748**	0.167	0.280	0.040
Gonion (G) $_{\text{Right}-\text{Left}}$	**0.872**	− 0.092	0.184	**0.912**
Tragion (T)-Pronasale (TP)	0.065	**0.947**	0.094	0.185
Menton (M)-Tragion (T)	0.127	0.299	− 0.056	0.310
Menton (M)- Gonion (G)	0.060	**0.882**	0.230	0.081
Tragion (T)-Gonion (G)	**0.604**	0.374	− 0.321	0.105

Extraction method: Principal component analysis. Rotation method: Varimax with Kaiser Normalization. Factor loadings greater than 0.40 were shown in bold typeface

Table 3 Rotated component matrix with highly loaded variables retained

Key variables	Component		
	1	2	3
Pronasale (TP)-P	0.220	**0.567**	0.088
P-Menton (M)	0.375	**0.659**	0.295
Menton (M)-Gonion (G)	0.135	**0.595**	− 0.100
P- Tragion (T)	**0.828**	− 0.195	0.221
Tragion (T)-Pronasale (TP)	**0.852**	− 0.133	0.199
Tragion (T)- Gonion (G)	**0.786**	0.210	− 0.117
Infraorbital (I)-P	0.283	− 0.174	0.317
Menton (M)-Tragion (T)	0.326	− 0.166	**0.476**

Factor loadings greater than 0.40 are shown in bold typeface

those variables (i.e., P-T, T-TP, T-G, TP-P, P-M, and M-G) were considered as key facial measurements.

Digital humans' classification through two-step cluster sampling

To examine RQ2, the key facial measurements were analyzed in terms of sex, ethnicity, and BMI, One-way ANOVA was used to find if these variables could be considered as factors for classifying digital humans for facemask sizing. No significant mean differences were found between each facial key measurement and sex ($df = 1$, $p > 0.05$). In contrast, significant mean differences were found between some of the key facial measurements and digital humans' BMIs and ethnicities (Tables 4 and 5). The M-G, P-T, and T-TP measurements were significantly different among participants in varying BMIs ($df = 3$, $p < 0.05$), but measurements including T-G, P-TP, and P-M did not show any significant mean differences ($df = 3$, $p > 0.05$). All the measurements except M-G were significantly different among participants in varying ethnicities ($df = 2$, $p < 0.05$).

Due to the significant mean differences between some of the key variables and digital humans' BMIs and ethnicities, both were considered the main factor for categorizing

Table 4 Statistical comparison between the key variables and digital humans' BMIs

Key variables	Sum of squares	df	Mean Square	F	Sig
P-Tragion (T)	295.11	3	98.37	2.932	0.045*
Tragion (T)- Pronasale (TP)	326.31	3	108.77	2.946	0.044*
Tragion (T)- Gonion (G)	49.59	3	16.53	0.840	0.480
Pronasale (TP)-P	11.14	3	3.71	0.619	0.607
P- Menton (M)	1.41	3	0.47	0.012	0.998
Menton (M)-Gonion (G)	387.40	3	129.13	6.726	< 0.001*

*$p < 0.05$

Table 5 Statistical comparison between the key variables and digital humans' ethnicity

Key variables	Sum of squares	df	Mean square	F	Sig
P-Tragion (T)	292.03	2	146.01	4.45	0.018*
Tragion (T)-Pronasale (TP)	435.25	2	217.62	6.52	0.003*
Tragion (T)-Gonion (G)	295.21	2	147.60	11.17	< 0.001*
Pronasale (TP)-P	36.13	2	18.06	3.41	0.042*
P-Menton (M)	453.36	2	226.68	7.91	0.001*
Menton (M)-Gonion (G)	112.05	2	56.02	2.20	0.124

*$p < 0.05$

Table 6 Final clusters and statistical analysis based on BMI and ethnicity

Key variables		Final cluster centers (mm)					ANOVA		
		1	2	Mean diff	Average	SD	df	F	Sig
Width	P-Tragion (T)	111.76	117.21	5.45	113.50	6.24	1	11.99	0.001*
	Tragion (T)-Pronasale (TP)	116.99	121.92	4.93	118.20	6.53	1	17.88	< .001*
	Menton (M)-Gonion (G)	89.10	94.03	4.93	90.47	5.23	1	9.18	0.004*
Length	Tragion (T)-Gonion (G	32.54	37.21	4.67	33.12	4.43	1	20.84	< .001*
	Pronasale (TP)-P	20.57	22.36	1.79	21.07	2.41	1	5.26	0.027*
	P-Menton (M)	103.89	109.29	5.40	103.74	6.17	1	19.36	< .001*

*$p < 0.05$

digital humans. A two-cluster model was found to be the most efficient and appropriate to represent the complexity among digital humans (cluster 1: n = 31, 72%, cluster 2: n = 12, 28%). The Black/African American digital humans were assigned to cluster 2, the White digital humans were assigned to cluster 1, most Asian digital humans were assigned to cluster 1 (n = 10, 83%), and the remaining were assigned to cluster 2 (n = 2, 17%). In terms of BMI, cluster 1 contained all the underweight (n = 3), 77% of the healthy weight (n = 20), 71% of the overweight (n = 5), and 43% of the obese digital humans, while cluster 2 contained 23% of the healthy weight (n = 6), 29% of the overweight (n = 2), and 57% of the obese (n = 4) digital humans. The final cluster of centroids presented in Table 6 was considered as the key measurements for developing the size range of the prototype face mask. Cluster 1 represented the digital humans having smaller measurements and cluster 2 represented the larger ones.

One-way ANOVA was conducted based on the 95% confidence level to compare the means of the six variables that were used in the cluster analysis. The overall F for the one-way ANOVA was statistically different ($p < 0.05$) among the width (i.e., P-T, T-TP, and M-G) and length (i.e., T-G, TP-P, and P-M) measurements. However, as can be seen in Table 6, the measurement differences between the means of clusters 1 and 2 were very small (~ 5.00 mm) to be considered as different sizes. Therefore, the average mean was used as a reference for adjusting the initial patterns of the cloth face mask. As shown in Fig. 4, the length of the center front panel (P-M) was shortened to 103.74 mm. Similarly, the length of T-G was shortened to 33.12 mm. While changing the length-related measurements, changes have been made to the length of lines related to the width measurements such as P-T = 113.50 mm, T-TP = 118.20 mm, and M-G = 89.10 mm.

Fit analysis

Subjective fit evaluation of the selected face mask design

Analyses of the fit rates showed that the novel face mask design provided an acceptable fit among 80% of the digital humans (n = 35). Twenty percent of the scans (n = 9) that received a not acceptable fit had very small ease at either mouth or nose or both levels. Girls received the most frequent acceptable fit ratings (n = 22, 50%) as compared to boys (n = 13, 29%). However, there were no significant mean differences between fit ratings and sex (X^2 (1, N = 44) = 2.57, $p = 0.116$). The acceptable fit was mostly observed among the digital humans with healthy weight BMI status (n = 21, 48%), followed by overweight (n = 6, 14%), obese (n = 6, 14%), and underweight (n = 2, 4%). The not acceptable fit was mostly observed among digital humans with healthy weight status (n = 6, 14%). However, no significant mean difference was observed between the fit ratings and digital humans'

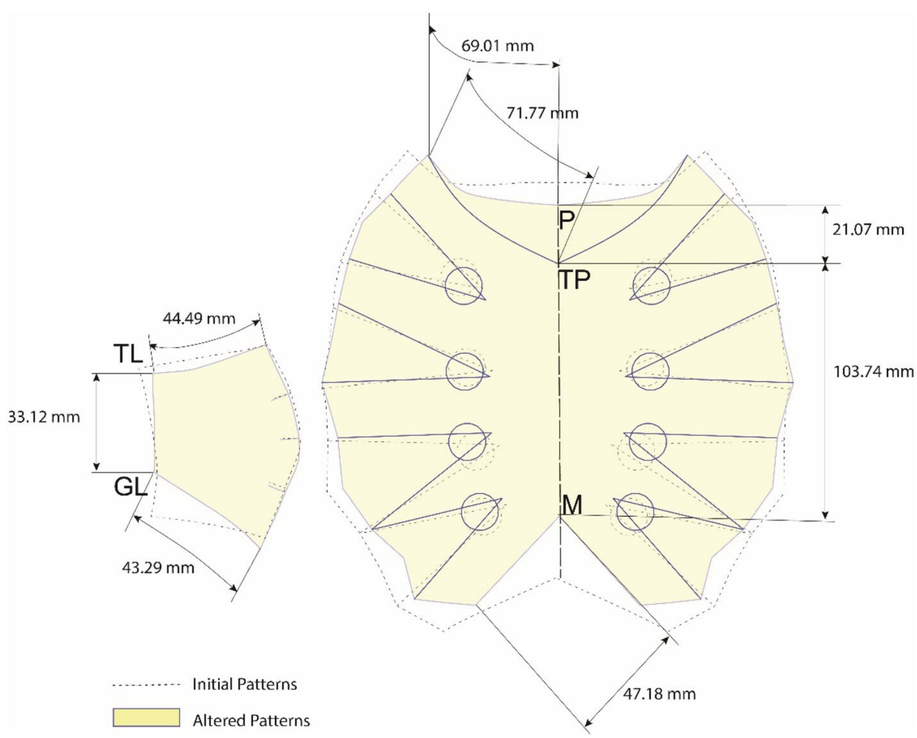

Fig. 4 The comparison of the initial patterns to the final patterns, which were altered based on digital humans' anthropometric data. Dart intakes were used to create pleats

BMIs (X^2 (3, N = 44) = 0.211, $p = 0.888$). A significant mean difference was observed among fit ratings and digital humans' ethnicities (X^2 (2, N = 44) = 19.14, $p < 0.001$). A post hoc Tukey test showed that the Black/African American digital humans differed significantly at $p < 0.05$ compared with the other two groups; Black/African American digital humans were the majority (n = 7, 16%) who received a not acceptable fit rating.

Objective fit evaluation of the selected face mask design

Measuring the distances between the digital humans' mouth, nose, and the inner layer of the face mask at the sagittal plane and tabulating them with the subjective fit ratings showed that on average, 22.58 mm ($SD = 11.53$ mm) ease at the mouth and 8.40 mm ($SD = 10.63$ mm) ease at the nose levels provided an acceptable fit. At the mouth level, boys had a smaller ease amount (i.e., shorter distance) ($M = 14.95$ mm) as compared to girls ($M = 21.28$ mm). However, these distances were not significantly different between sexes ($F = (1, 43) = 2.577$, $p = 0.122$). Digital humans in the obese category had a longer distance at the mouth level ($M = 20.84$ mm) as compared with the ones in the healthy weight ($M = 18.72$ mm), overweight ($M = 17.57$ mm), and underweight ($M = 13.07$ mm) categories. However, the distances were not significantly different among the BMI groups (F (3, 43) = 0.239, $p = 0.869$). In terms of ethnicity, significant mean differences were found for the ease between the mouth and the inner layer of the prototype face mask ($F = (2, 43) = 7.37$, $p < 0.001$). A post hoc Tukey test showed that the differences are mainly between Black/African American and White digital humans, and Black/African American and Asian digital humans, while no significant mean difference was observed between White and Asian digital humans. For Black/African American digital humans, the average ease at the mouth level was smaller ($M = 6.25$ mm) as compared with Asian ($M = 20.68$ mm), and White ($M = 22.81$ mm) digital humans (Table 7).

At the nose level, boys had smaller average ease ($M = 6.73$ mm) as compared to girls ($M = 7.76$ mm). However, the recorded distances between the nose tip and face mask were not significantly different among sex groups (F (1, 43) = 0.110, $p = 0.742$). Also, digital humans in the obese category had bigger ease at the nose level ($M = 9.46$ mm) as compared to those in the healthy weight ($M = 7.56$ mm), overweight ($M = 6.77$ mm), and underweight ($M = 1.33$ mm) categories. However, the distances/ease amounts were not significantly different among the four BMI groups ($F = (3, 43) = 0.486$, $p = 0.694$). In terms of ethnicity, White digital humans ($M = 13.06$ mm) had longer distances (ease)

Table 7 Comparison of objective and subjective fit evaluations at the mouth level based on digital humans' ethnicity

		Ease at the mouth level (mm)				Subjective fit evaluation
Ethnicity	**n (%)**	**Mean**	**SD**	**Min**	**Max**	
Asian	11 (25%)	22.48	12.64	5.37	41.4	Acceptable
	1 (2%)	0.08	0.00	0.80	0.80	Not acceptable
Black/African American	3 (7%)	15.01	11.70	1.72	23.8	Acceptable
	7 (16%)	2.50	9.47	0.71	4.60	Not acceptable
White	21 (48%)	23.70	11.07	6.35	56.99	Acceptable
	1 (2%)	4.03	0.00	4.03	4.03	Not acceptable

at the nose level as compared with Asian ($M=8.64$ mm), and Black/African American ($M=2.27$ mm) digital humans. However, no significant mean differences were found for the distance between the nose and the inner layer of the face mask among ethnic groups ($F=(2, 43)=1.65$, $p=0.204$). The digital humans who received a not acceptable fit rating (n = 9, 25%) had an average of 2.95 mm ($SD=2.30$ mm) ease at their nose and an average of 2.47 mm ($SD=1.41$ mm) at their mouth levels.

Discussion

As the world continues to adapt to living in a new reality that may require wearing masks when Covid-19, or similar, cases increase, it is important to provide children with well-fitted and comfortable facemasks. This study focused on developing digital methods to examine the sizing and fit of a novel cloth face mask design by using 44 head scans of 6-year-olds from the Size North America database. Its purpose was to provide guidelines for designing a well-fitted cloth face by examining children's facial anthropometry, how it contributes to developing size groups for an effective face covering for protection, and how facemask fit can be evaluated digitally based on facial and facemask landmarks (Fig. 5).

Concerning the first research question, the study findings showed that two PCs represented the important measurements to be taken into consideration when sizing face masks to achieve good fit and protection. Width measurements including P-T, T-TP, and M-G, and length measurements including T-G, TP-P, and P-M were found to be the most critical key measurements. This finding is similar to the findings from Goto et al.'s (2015) study that analyzed the 3D anthropometric data set for designing ventilation masks among 6 years old children (N = 65) and highlighted the importance of two PCs including width- and length-related measurements as input for improving sizing

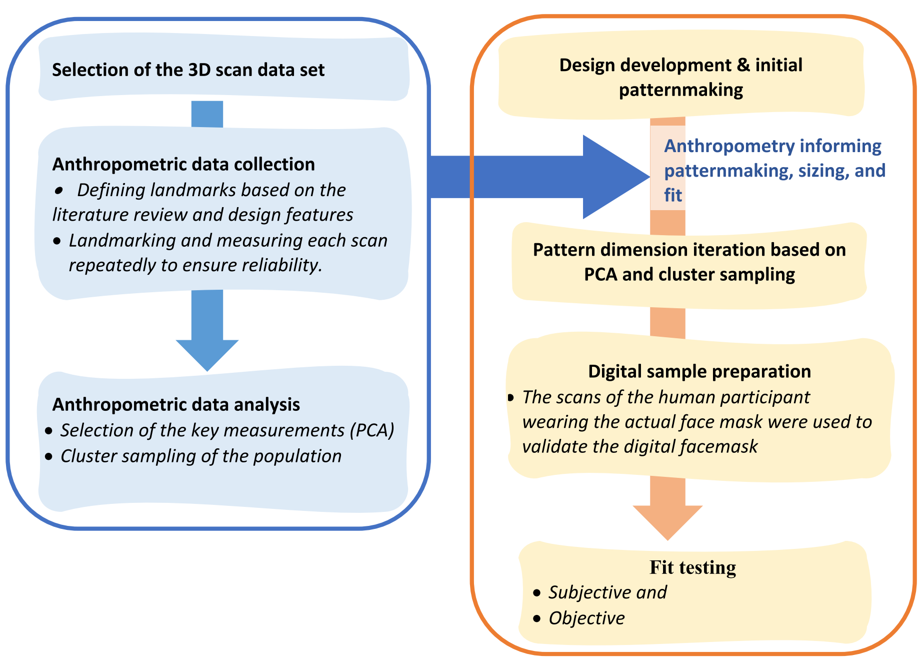

Fig. 5 A summary of the methods developed and used in the study for face mask sizing and digital fit analysis

approaches. However, Goto et al. (2015) applied different landmarks than the ones used in the present study due to the narrower design and smaller area coverage of the ventilation mask. In our study, we considered the cloth facemask's sealing point on the nose bridge and included additional landmarks such as tragion, gonion, and infraorbital. Therefore, the present study is valuable because its focus was on one age group and identified critical measurements for the optimal fit of another product, i.e., cloth face mask fit.

For the second research question, BMI and ethnicity were found to be the main factors for identifying the size range. BMI was significantly different among all the width-related measurements whereas ethnicity was significantly different among all three length- and two width-related measurements. M-G (width measurement) was not significantly different among the ethnicities. Children with higher BMIs would need a bigger size face mask than the one-size-fits-all type of face mask. Ethnicity would also be important when developing size ranges. Black/African American digital humans' face measurements were found to be bigger than the other two groups' measurements. When digitally trying-on the face mask, the average ease at the mouth level was significantly smaller than the ease measured on the Asian and White digital humans' faces. Ethnicity is a known factor that influences growth (Churchill et al., 1978; Farkas et al., 2005). In this regard, results from digital fit testing indicated the importance of considering the differences in facial topologies among ethnicities when creating unisex face mask designs. However, due to the small sample size, we cannot extend or generalize our findings. Sex was not found to be a key factor in improving the fit of cloth face mask prototype for 6 years old children. This finding was also consistent with findings from the study of the variation in 3D face shapes of Dutch children for mask design (Goto et al., 2021), stating that when considering anthropometric data of children of a certain age range for applications in product design, sex can often be combined. As suggested by Bradtmiller, (1996) and Goto et al. (2019), sex-combined data can be more helpful when designing unisex products such as a facemask.

Related to the third research question, to analyze the fit of the face mask simulations on the digital humans' scans, objective measurements of the face mask's distance to the nose and mouth levels as well as subjective evaluations related to the overall fit of the face mask were used together. Analyzing statistical data helped with defining a good/acceptable fit for the selected cloth face mask and associating it with ease amounts. To take the distance measurements from the scans, horizontal and vertical cross-sections were created on the scans, which were wearing digital face masks. For an acceptable fit rating, the study's findings suggested providing a 22.58 mm ease amount at the mouth and an 8.40 mm ease amount at the nose levels on the sagittal plane. As the face mask fit was designed based on the facial anthropometric data obtained from 3D scans, most of the digital humans (n = 35, 80%) received acceptable fit ratings and only twenty percent (n = 9) of the digital humans had a tight fit at the nose and mouth. Even though the BMI groups had significant differences in face dimensions, mask fit was not different among them. This could be because more than half of the digital humans (61%) were in the normal BMI category and the maximum facial key measurement differences (~ 10 mm) among BMI categories did not generate a fit concern for the expert judges during subjective fit analysis. The key facial measurements were significantly different among the ethnicities and the subjective fit analysis determined that Black/African American digital humans had a significantly tighter fit at the mouth level. The objective fit evaluations identified that Black/African American digital humans had significantly small ease at the mouth level compared with other ethnic groups but at the nose, there was not any significant difference. The maximum difference among key facial measurements that were significant difference among the ethnicities (~ 7 mm) and the fit issues generated by wearing the same digital facemask were detected by the expert judges. This could be attributed to facial shape differences in addition to measurement differences. It is plausible that digital humans' facial shape variations such as prominent cheeks and nose, may have caused this finding. The study findings hinted at the importance of considering measurements' relations (i.e., shape information such as nose and mouth protrusions on the sagittal plane) as supplemental data when designing a cloth-face mask. As previous work from body-related studies has shown (Petrova & Ashdown, 2008), the fit is not only affected by measurements, but also by shapes (i.e., how measurements relate to each other). Therefore, conducting a facial shape analysis among children, especially in different BMI and ethnic categories, would be immensely useful to design better-fitting cloth facemasks.

This study had several additional limitations; therefore, results should be taken into consideration carefully when interpreting the findings. Because of the difficulty in recruiting participants for face scan research during the pandemic, the novel cloth-face mask prototype was only tested on 3D scans of children from an existing database. Follow-up studies should also include recruiting children to compare our findings to the actual wear conditions with subjective comfort evaluations from participants. Using the digital files from the same age range helped control the age variable, however, the heterogeneous sample size was a limitation to generalizing study findings. The participants were mostly in the healthy-weight category and of White ethnicity, therefore the present study could be considered as a case study for developing guidelines in digital sizing and fit analysis for facemasks. Some of the scan files were not useable for virtual fittings because the subject was captured by making a facial expression during scanning. Due to the limited access to the Size North America database, the number of scans used in this study was small. Therefore, the findings may not be generalizable and should be used cautiously when extending to a larger sample of children even within the same age group (6 years old). This study used Size North America data as the latest representative facial dimension data of the children in the USA. Further studies should use larger databases by repeating applied methods to translate anthropometric data from diverse ethnicities and BMI to the product design. The face mask tried on the scans was a digital simulation and may not reflect the actual drape of the facemask with full accuracy. Nonetheless, the present study findings suggested some future steps that must be taken into consideration when characterizing the facial measurements design of a cloth face mask optimized for fit.

Conclusions

3D body scanning technology and digital models have become invaluable tools for evaluating product fit and determining optimal sizing. In this study, a novel face mask design was assessed using head scans from a group of 6-year-old boys and girls and validated the use of digital forms in this context. In addition to providing step-by-step guidelines applied to the sizing and fit analysis of a facemask design for a given digital database of head scans, the study highlighted the fact that BMI and ethnicity should be considered when sizing the face masks. Findings also indicated that designers should consider the measurements taken in the sagittal view for facial proportions and the relations of the nose and mouth protrusions at the sagittal plane variations. More research on children's facial shape variations in different age groups would help with a better understanding of the facial variations and improving the fit of the face masks. Also, if the end use of a face mask is different it could potentially affect its design requirements, thus the placement of landmarks on the face. Landmarks are reference points that guide the proper fit and positioning of a face mask. The fit and effectiveness of the mask may be compromised if landmarks are not aligned with the mask design. These considerations highlight the multifaceted nature of face mask design and the significance of a tailored approach to achieve an optimal and secure fit for all users.

Acknowledgements
The authors would like to thank Human Solutions of North America, Inc. for their collaboration. We would also like to thank the Cornell Statistical Consulting Unit staff for their support. Our belated thanks go to P.A.O., who was the human participant in our first manuscript of this series, for his help and patience throughout numerous head scanning and face mask fit sessions.

Authors' contributions
MM acquired the head scan database, developed the sizing of the face mask, conducted landmarking and data analysis, evaluated the face mask fit, and wrote the manuscript. JLDP designed experimental masks that were used for developing digital prototypes. KG and JLDP contributed to the project conceptualization and draft preparation, reviewing, and editing of the manuscript. MF guided manuscript reviewing and revising and supervised the overall project. HTP guided manuscript reviewing, and revising, acquired funding, and supervised the overall project. FB guided manuscript writing, reviewing, and revising, evaluated the face mask fit, and supervised the overall project. All authors read and approved the final manuscript.

Funding
This work is/was partially supported by two Cornell Atkinson Center for Sustainability Covid-19 Rapid Response Fund grants, as well as the National Institute of Food and Agriculture, U.S. Department of Agriculture, Hatch/Multi-State under #1017350. Any opinions, findings, conclusions, or recommendations expressed in this publication are those of the authors and do not necessarily reflect the view of the National Institute of Food and Agriculture (NIFA) or the United States Department of Agriculture (USDA).

Availability of data and materials
All data is available via the Fashion and Body Tech Lab and archived electronically on Cornell Box.

Declarations

Ethics approval and consent to participate
Human Solutions had consent forms for the participants and parents signed the forms on behalf of their children before body scanning. The company shared the dataset with our research team after anonymizing and de-identifying the data. The scans were analyzed as secondary data. Scanning one participant upon receiving approval from his parents to establish a baseline for a virtual facemask did not require IRB review as the activity did not meet the definition of human subjects research.

Competing interests
None of the authors have any competing interests.

Received: 13 February 2023 Accepted: 16 November 2023
Published online: 25 January 2024

References

3M. (2021). *Filtering Facepiece Respirators FAQ: General Public* [Technical Bulletin]. https://multimedia.3m.com/mws/media/1791526O/respiratory-protection-faq-general-public-tb.pdf

American Academy of Pediatrics. (2022, January 10). *Face Masks*. https://www.aap.org/en/pages/2019-novel-coronavirus-covid-19-infections/clinical-guidance/cloth-face-coverings/

American Association of Textile Chemists and Colorists. (2020). Guidance and considerations for general purpose textile face coverings: Adult. AATCC M14-2020, 446–450.

Amirav, I., Luder, A. S., Halamish, A., Raviv, D., Kimmel, R., Waisman, D., & Newhouse, M. T. (2014). Design of aerosol face masks for children using computerized 3D face analysis. *Journal of Aerosol Medicine and Pulmonary Drug Delivery, 27*(4), 272–278. https://doi.org/10.1089/jamp.2013.1069

Ashdown, S. P., Loker, S., & Rucker, M., & Davis, U.C. (2005). *Improved apparel sizing: Fit and anthropometric 3-D scan data.* Technical report, (No. S04-CR01 National Textile Center).

Ashdown, S. P., Loker, S., Schoenfelder, K., & Lyman-Clarke, L. (2004). Using 3D scans for fit analysis. *Journal of Textile and Apparel, Technology and Management, 4*(1), 1–12.

Asociacion RUVID (2020). (2022, February 20). *Mask measurements established for children aged 3 to 12*. Medical Xpress. https://medicalxpress.com/news/2020-05-mask-children-aged.html

Bradtmiller, B (1996). Sizing head forms: Design and development. *SAE transactions*, 443–450.

Centers for Disease Control and Prevention (n.d.). (2021, February 16). *BMI Percentile Calculator for Child and Teen*. https://www.cdc.gov/healthyweight/bmi/calculator.html

Centers for Disease Control and Prevention. (2022). Use and Care of MasksUse and Care of Masks. Retrieved August 15, 2022 from https://www.cdc.gov/coronavirus/2019-ncov/prevent-getting-sick/about-face-coverings.html

Churchill, E., Laubach, L.L., Mcconville, J.T., Tebbetts, I., 1978. Anthropometric Source Book. Volume 1: Anthropometry for Designers. NASA, Houston, Tex., United States.

Conkle, J., Keirsey, K., Hughes, A., Breiman, J., Ramakrishnan, U., Suchdev, P. S., & Martorell, R. (2019). A collaborative, mixed-methods evaluation of a low-cost, handheld 3D imaging system for child anthropometry. *Maternal & Child Nutrition, 15*(2), Article e12686. https://doi.org/10.1111/mcn.12686

Du Puis, J. L., Forstenhausler, L., Goodge, K., Maher, M., Frey, M., Baytar, F., & Park, H. (2022). Cloth face mask fit and function for children part one: Design exploration. *Fashion and Textiles, 9*(1), 14. https://doi.org/10.1186/s40691-022-00287-8

Erwin, M. D., Kinchen, L. A., & Peters, K. A. (1979). *Clothing for moderns*. Macmillan.

Fan, J., Yu, W., & Hunter, L. (2004). *Clothing appearance and fit: Science and technology*. Woodhead publishing.

Farkas, L. G., Katic, M. J., & Forrest, C. R. (2005). International anthropometric study of facial morphology in various ethnic groups/races. *The Journal of Craniofacial. Surgery., 16*(4), 615–646. https://doi.org/10.1097/01.scs.0000171847.58031.9e

Farkas, L. G., Posnick, J. C., & Hreczko, T. M. (1992). Anthropometric growth study of the head. *The Cleft Palate-Craniofacial Journal, 29*(4), 303–308. https://doi.org/10.1597/1545-1569_1992_029_0303_agsoth_2.3.co_2

Fenlon, R. (2007). Facial Respirator Shape Analysis using 3D Anthropometric Head Data. In: NIST Interagency/Internal Report (NISTIR), *National Institute of Standards and Technology*, Gaithersburg, MD, [online]. Retrieved February 20, 2021, from https://tsapps.nist.gov/publication/get_pdf.cfm?pub_id=51230

Ferrario, V. F., Sforza, C., Poggio, C. E., & Schmitz, J. H. (1998). Facial volume changes during normal human growth and development. *The Anatomical Record* An OfficialPublication of the American Association of Anatomists *250*(4), 480-487.

Fu, F., & Luximon, Y. (2019). Head and face anthropometric study for Chinese children. *Industrial Engineering & Management Systems, 18*(4), 619–629. https://doi.org/10.7232/iems.2019.18.4.619

Fu, F., Luximon, A., & Luximon, Y. (2019). A comparison of traditional and 3D scanning measurement in ear anthropometry. *International Conference on Applied Human Factors and Ergonomics*, 417–423. https://doi.org/10.1007/978-3-030-20142-5_42

Gill, S. (2015). A review of research and innovation in garment sizing, prototyping and fitting. *Textile Progress, 47*(1), 1–85. https://doi.org/10.1080/00405167.2015.1023512

Goodge, K., Du Puis, J. L., Maher, M., Frey, M. W., Baytar, F., & Park, H. (2022). Cloth face mask fit and function for children part two: Material selection. *Fashion and Textiles, 9*(1), 1–18. https://doi.org/10.1186/s40691-022-00315-7

Gordon, C. C., Blackwell, C. L., Bradtmiller, B., Parham, J. L., Barrientos, P., Paquette, S. P., Corner, B. D., Carson, J. M., Venezia, J. C., & Rockwell, B. M. (2014). *2012 anthropometric survey of us army personnel: Methods and summary statistics*.

Goto, L., Lee, W., Huysmans, T., Molenbroek, J. F., & Goossens, R. H. (2021). The variation in 3D face shapes of dutch children for mask design. *Applied Sciences, 11*(15), Article 6843. https://doi.org/10.3390/app11156843

Goto, L., Lee, W., Molenbroek, J. F., Cabo, A. J., & Goossens, R. H. (2019). Traditional and 3D scan extracted measurements of the heads and faces of Dutch children. *International Journal of Industrial Ergonomics, 73*, Article 102828. https://doi.org/10.1016/j.ergon.2019.102828

Goto, L., Lee, W., Molenbroek, J., & Goossens, R. (2015). Analysis of a 3D anthropometric data set of children for design applications. *In Proceedings 19th Triennial Congress of the IE*. Vol. 9. 2015.

Lee, J., & Lee, W. (2021). Analysis of head dimensions of Korean children and adolescents for ergonomic product design. *Journal of the Ergonomics Society of Korea*, 162–162.

Lin, A. J., Lai, S., & Cheng, F. (2010). Growth simulation of facial/head model from childhood to adulthood. *Computer-Aided Design and Applications, 7*(5), 777–786. https://doi.org/10.3722/cadaps.2010.777-786

Loker, S., Ashdown, S., & Schoenfelder, K. (2005). Size-specific analysis of body scan data to improve apparel fit. *Journal of Textile and Apparel, Technology and Management, 4*(3), 1–15. https://textiles.ncsu.edu/tatm/wp-content/uploads/sites/4/2017/11/Loker_full_136_05.pdf

Napolitano, N., Nishisaki, A., Buffman, H. S., Leffelman, J., Maltese, M. R., & Nadkarni, V. M. (2017). Redesign of an open-system oxygen face mask with mainstream capnometer for children. *Respiratory Care, 62*(1), 70–77. https://doi.org/10.4187/respcare.04751

Petrova, A., & Ashdown, S. P. (2008). Three-dimensional body scan data analysis: Body size and shape dependence of ease values for pants' fit. *Clothing and Textiles Research Journal, 26*(3), 227–252. https://doi.org/10.1177/0887302X07309479

Seo, H., Kim, J. I., Yoon, J.-S., Shin, D., & Kim, H. (2017). Analysis of 3D facial dimensions and pulmonary capacity of Korean children for designing of children's dust masks. *Journal of Korean Society of Occupational and Environmental Hygiene, 27*(4), 269–282. https://doi.org/10.15269/JKSOEH.2017.27.4.269

Smart, N. R., Horwell, C. J., Smart, T. S., & Galea, K. S. (2020). Assessment of the wearability of facemasks against air pollution in primary school-aged children in London. *International Journal of Environmental Research and Public Health, 17*(11), 3935. https://doi.org/10.3390/ijerph17113935

Snyder, A. M., Weisel, H. L., & Chatfield, S. L. (2020). Mobilizing communities to sustainably produce face masks: Public health practice in the time of COVID-19. *Ohio Journal of Public Health, 3*(2), 25–29. https://doi.org/10.18061/ojph.v3i2.9013

Spanish Association for Standardization- UNE. (2020). UNE 0064–2:2020. *Non-reusable hygienic masks. requirements of materials, design, manufacturing, marking and use.* Part 2: For children use.

U.S. Census Bureau (2022). (2022 March 15). *About the topic of race.* https://www.census.gov/topics/population/race/about.html

Weatherbed, J. (2023). *Levi's will test AI-generated clothing models to 'increase diversity.* https://www.theverge.com/2023/3/27/23658385/levis-ai-generated-clothing-model-diversity-denim

Zhuang, Z., Benson, S., & Viscusi, D. (2010). Digital 3-D head forms with facial features representative of the current US workforce. *Ergonomics, 53*(5), 661–671. https://doi.org/10.1080/00140130903581656

Publisher's Note

Springer Nature remains neutral with regard to jurisdictional claims in published maps and institutional affiliations.

Mona Maher Ph.D. student at Department of Human Centered Design, College of Human Ecology Cornell University, Ithaca, NY14853, USA.

Jenny Leigh Du Puis Ph.D. student at Department of Human Centered Design, College of Human Ecology Cornell University, Ithaca, NY 14853, USA.

Katarina Goodge Ph.D. student at Department of Human Centered Design, College of Human Ecology Cornell University, Ithaca, NY 14853, USA.

Margaret Frey Professor at Department of Human Centered Design, College of Human Ecology Cornell University, Ithaca, NY14853, USA.

Heeju Terry Park Associate Professor at Department of Human Centered Design, College of Human Ecology Cornell University, Ithaca, NY 14853, USA.

Fatma Baytar Assistant Professor at Department of Human Centered Design, College of Human Ecology Cornell University, Ithaca, NY 14853, USA.